sciendo

DOI: 10.2478/auoc-2024-0015

Ovidius University Annals of Chemistry Volume 35, Number 2, pp. 111 - 117, 2024

Thermal-hydraulic analysis of a louver fin-and-tube radiator for a liquid–cooled PEMFC stack system

Viorel IONESCU*

Department of Physics and Electronics, Ovidius University of Constanta, 124 Mamaia Blvd., 900527 Constanta, Romania

Abstract. The present study aimed to develop a parametric analysis from the perspective of heat transfer and dimensionless pressure drop for a cross-flow heat exchanger with louvered fins and flat tubes. Four different radiator core models were considered here, with specific values of geometrical parameters as selected from the manufacturer's datasheets. Effectiveness – the NTU (Number of Transfer Units) method was used to evaluate the total heat flux transferred between the cold and hot sides of the radiator. A possible application of the designed louvered fin radiator can be as a part of a liquid–cooling system for an automotive Proton Exchange Membrane Fuel Cell (PEMFC) stack with coolant flow rates of 1 l/min and 2 l/min, frontal air velocities up to 14 m/s and inlet temperatures for the coolant and air side of 343 K and 298 K, respectively. One of the radiator models investigated, having the lowest louver pitch to fin pitch ratio, highest fin length to fin pitch ratio and lowest louver length, showed the best thermo–hydraulic performance, with the highest surface goodness factor values along the entire Reynolds number domain.

***Keywords*:** louvered fins; friction factor; Colburn factor; heat rejection rate.

1. Introduction

Louver fin–and-tube radiators are used on a large scale in the automotive industry, presenting superior heat transfer efficiency [1, 2]. The liquid flux circulating through the radiator tubes is effectively cooled under the convective heat transfer established at the contact area between the air flux and louver fins. The heat transfer rate of this type of radiator is enhanced due to complex airflow patterns formed at the boundary of louvre fins with interrupt surfaces [3].

Several studies reported in the literature the thermal performance of radiators with louvred fins and other types of fins. Experimental results published by Habibian and Abolmaali [4] indicated that the louvered fin radiator improved the heat transfer rate by 24.6 % in comparison with plain fin radiator. This enhancement was obtained under the 67.7 % air–side pressure drop increase. After extending the flow path, a pressure drop increase is always expected for louver fins. Another comparative study was reported by Wang et al. [5] for fin – and–tube heat exchangers with plain, louvre and semi–dimple vortex generator (VG) type fins. The heat transfer coefficient of the radiator with louver fins increased by about 2 % -15 % compared to VG–type radiators. Overall, the louvre fins present a higher capacity to dissipate heat [6, 7].

Although the thermal performance of louvre fins is higher than that of the other types of fins, it is necessary to attain the biggest possible heat transfer improvement while maintaining the minimum pressure drop under the heat exchanger design [8]. This target can be fulfilled by optimizing some key geometrical parameters of the radiator. The contribution of the geometrical parameters that influence the thermal–hydraulic performance of the louvred fin radiator was analyzed by Qi et al. [9] using the Taguchi method. They observed that the most critical parameters are the flow depth, fin pitch, fin thickness and number of louvers, with contributions of about 31%, 21% and 20%, respectively. Tube pitch and louver angle can also play an essential role in the heat exchanger design, with contributions of 13%. A. Okbaz et al. [10] emphasized the impact on the radiator's thermo-hydraulic performance presented by the fin length to fin pitch ratio, respectively, louver pitch to fin pitch ratio, in correlation with the louvre length and louvre angle.

A proper design and analysis of the radiator is developed through the knowledge of the dimensionless form for the heat transfer coefficient. Generally, the dimensionless heat transfer properties are expressed in terms of the Colburn factor, j, versus the Reynolds number, Re. Another performance parameter is the friction factor, f, which is the dimensionless form of the pressure drop for the external air side of the radiator. In the case of heat exchangers designed with applications in automotive cooling systems, the general thermo-hydraulic performance can be evaluated through the "surface goodness factor" j/f [11] or through the "volume goodness factor" $j/f^{1/3}$ [12], terms which include both the j and the f factors and presents with higher precision the desired cooling performance.

An exciting application of the louvered fin radiator, used in the cross-flow configuration of coolant tubes and air fins, can be as a part of the liquid-cooled system for

E-mail address: v_ionescu@univ-ovidius.ro (Viorel Ionescu)

the proton exchange membrane fuel cell (PEMFC) vehicles like Microcab H2EV [13] or Suzuki Burgmann fuel cell scooter [14]. Heat is removed from the fuel cell stack by a water/glycol mixture under forced convection. This coolant flux circulates through the circular channels of the stack bipolar plates in a closed loop containing also the coolant tank, a coolant pump with variable flow rate, a by-pass valve for the stack temperature regulation via feedback control and the radiator with air cooling under forced convection [15].

In the present study, four different models of the fin-and-tube radiator core were analyzed by modifying various louver/fin geometrical parameters from one model to another. The ultimate objective of this investigation was to establish the core model geometry, which presents the highest heat rejection rate and the minimum flow resistance.

2. Methodology

2.1. Heat exchanger design

Geometrical design parameters for the core of a compact heat exchanger with corrugated fins and flat cooling tubes are presented in Fig. 1. We can see here that each of the fins is louvred to generate turbulent airflow and to enhance this way the heat transfer rate between the air and coolant fluxes. The louver and fin design will directly affect the radiator's airflow resistance and thermal performance. Cross-flow type geometry for the coolant and air was considered here (see Fig. 1).

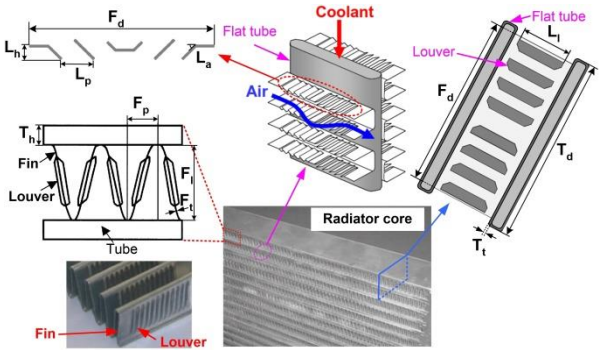

Figure 1. Geometry details of the cross-flow heat exchanger, with corrugated louver fins and flat tubes

Table 1 presents the design parameters for the louvred fin heat exchanger core with values considered from different datasheets [16]. The other geometrical parameters of the radiator, constant throughout this analysis, are: Louver height L_h = 0.315 mm; Tube length T_l = 382 mm; Tube height, T_h = 2.5 mm; Tube thickness T_t = 0.32 mm; Number of tubes N_T = 28 [17]. As we can see from Table 1, four different core models (M1 – M4) are studied here.

Table 1. Design parameters of the radiator [16]

Parameters	Models			
	M1	**M2**	**M3**	**M4**
Louver angle, L_a (mm)	16.5	21.5	**25.5**	30
Louver pitch, L_p (mm)	2.25	1.4	**1.1**	1.65
Louver length, L_l (mm)	7.1	8.5	**6.8**	7.09
Fin length, F_l (mm)	7.8	9	**9.6**	8.6
Fin thickness, F_t (μm)	75	50	**60**	157
Fin pitch, F_p (mm)	1.51	2.09	**1.8**	1.69
Tube depth, T_d (mm)	40	32	**50**	25.4

2.2. Thermo-hydraulic model description

Considering an even distribution of the coolant (50/50 water-glycol mixture) through each of the radiator flat tubes [15], we used here the Gnielinski correlation for the fully developed laminar flow regime (Re_{Dh} < 2300) to calculate the Nusselt number Nu_c, using the following equation [18]:

$$Nu_c = \left[\begin{array}{l} 4.354^3 + 0.6^3 + \left(\sqrt[3]{\mathrm{Re}_{Dh}\,\mathrm{Pr}_c\,D_h / T_l} - 0.6 \right)^3 + \\ + \left(0.924 \sqrt[3]{\mathrm{Pr}_c} \cdot \sqrt{\mathrm{Re}_{Dh}\,D_h / T_l} \right)^3 \end{array} \right]^{1/3} \quad (1)$$

In relation (1), the hydraulic diameter of the coolant tube is calculated as [5]: $D_{hc} = 2T_hT_d / (T_h + T_d)$.

Reynolds number for the cooling side, based on the hydraulic diameter, was determined with relation [19]:

$$\mathrm{Re}_{Dh} = \frac{2m_c}{(T_h + T_d)\mu_c} \quad (2)$$

where m_c is the coolant mass flow rate in kg/s and μ_c is the dynamic fluid viscosity (kg/m·s).

Prandl number for the cooling side, Pr_c, is calculated as:

$$\mathrm{Pr}_c = \frac{\mu_c \cdot c_{p,c}}{k_c} \quad (3)$$

were $c_{p,c}$ is the coolant specific heat capacity (J/kg·K), and k_c is the coolant thermal conductivity (W/m·K).

The heat transfer coefficient of the cooling fluid h_c (W/m^2·K) will be determined with the expression [20]:

$$h_c = \frac{Nu_c \cdot k_c}{D_{hc}} \quad (4)$$

The friction coefficient f_c on the cooling liquid side, for laminar flow, was calculated as [20]:

$$f_c = 64 / \mathrm{Re}_{Dh} \quad (5)$$

The heat transfer coefficient for the air side convection h_a (W/m^2·K) was calculated based on the relation [20]:

$$h_a = j \cdot \rho_a \cdot V_a \cdot c_{p,a} \cdot \mathrm{Pr}_a^{-2/3} \quad (6)$$

were ρ_a and V_a are the air density (kg/m^3) and velocity (m/s), respectively.

Prandl number for the air side Pr_a was defined by the expression:

$$\mathrm{Pr}_a = \frac{\mu_a \cdot c_{p,a}}{k_a} \quad (7)$$

with c_p as the air-specific heat capacity (J/kg·K), k_a as the air thermal conductivity (W/m·K) and μ_a as the dynamic air viscosity (kg/m·s).

In relation (6), j is the Colburn factor, calculated with the empirical correlation proposed by Chang and Wang [21]:

$$j = \mathrm{Re}_{Lp}^{-0.49} \cdot \left(\frac{L_a}{90}\right)^{0.27} \cdot \left(\frac{F_p}{L_p}\right)^{-0.14} \cdot \left(\frac{F_l}{L_p}\right)^{-0.29} \cdot \left(\frac{T_d}{L_p}\right)^{-0.23} \cdot \left(\frac{L_l}{L_p}\right)^{0.68} \cdot \left(\frac{F_l + T_h}{L_p}\right)^{-0.28} \cdot \left(\frac{F_t}{L_p}\right)^{-0.05} \quad (8)$$

The Reynolds number based on the louver pitch L_p is calculated as [22]:

$$\mathrm{Re}_{Lp} = \frac{\rho_a \cdot V_a \cdot L_p}{\mu_a} \quad (9)$$

The correlation (8) is applied for $30 < Re_{Lp} < 5000$ and predicts experimental j factors of 91 radiator cores within ±15 % (mean deviation of 8%) for louvered fin exchangers with the following geometrical parameter limits: $0.5 \leq L_p \leq 3$ mm; $8.4 \leq L_a \leq 35^o$; $0.51 \leq F_p \leq 3.3$ mm; $2.8 \leq F_l \leq 20$ mm; $15.6 \leq T_d \leq 57.4$ mm; $2.13 \leq L_l \leq 18.5$ mm and $7.51 \leq F_l + T_h \leq 25$ mm [23].

The air side friction coefficient (f_a) was calculated with the correlation proposed by Chang et al. [24], established for the same radiator core database as the j – factor, with similar accuracy:

$$f_a = f_1 \cdot f_2 \cdot f_3 \quad (10)$$

$$f_1 = 4.97\,\mathrm{Re}_{Lp}^{0.6049 - 1.064/L_a^{0.2}} \cdot \left(\ln\left(0.9 + \left(\frac{F_t}{F_p}\right)^{0.5}\right)\right)^{0.527} \quad (11)$$

$$f_2 = \left(\frac{D_{ha}}{L_p} \cdot \ln\left(0.3\,\mathrm{Re}_{Lp}\right)\right)^{-2.966} \cdot \left(\frac{F_p}{L_l}\right)^{-0.7931(F_l + T_h)/T_h} \quad (12)$$

$$f_3 = \left(\frac{F_l + T_h}{T_h}\right)^{-0.0446} \cdot \ln\left(1.2 + \left(\frac{L_p}{F_p}\right)^{1.4}\right)^{-3.553} \cdot L_a^{-0.477} \quad (13)$$

The friction coefficient correlation defined above is available for $150 < Re_{Lp} < 5000$.

The hydraulic diameter for louvered fin was calculated as [20]:

$$D_{ha} = \frac{2\left[\left(F_p - F_t\right) \times F_l\right]}{\left(F_p - F_t\right) + F_l} \quad (14)$$

Effectiveness – NTU (Number of Transfer Units) method was used here for the heat transfer rate evaluation.

Inside a virtual thermal circuit, we considered the tube – side thermal resistance as a contamination factor R_{th} and the fin wall resistance, along with the hot –side and cold –side thermal resistances. Thus, the overall thermal conductance U_0A_0 (W/K) can be expressed in the following form [25, 26]:

$$\frac{1}{U_a A_a} = \frac{1}{h_a A_a} + \frac{F_t}{k_f A_w} + R_{th} + \frac{1}{h_c A_c} \quad (15)$$

The global thermal resistance equation (15) presented above is available under the assumption of a heat exchanger without extended surface on either side, so the hot and cold surface effectiveness are unity and the average wall area $A_w = (A_c + A_a)/2$ [25].

In relation (15), the heat transfer area of the cooling fluid A_c (m^2) was calculated as [20]:

$$A_c = N_T \cdot \left(2T_h T_d + 2T_h T_l\right) \quad (16)$$

and the heat transfer area of the air-side, A_a (m^2), was given by relation [20]:

$$A_a = \left\{\left[F_t \cdot \left(F_l - L_l\right) + L_l L_h\right] \cdot N_F\right\} \cdot \left(N_T + 1\right) \quad (17)$$

For a core width W = 635 mm [17], the total number of fins from the core was calculated with relation [23]:

$$N_F = N_P \frac{W}{F_p} \quad (18)$$

N_p = 2 is the number of finned passages.

The contamination factor R_{th} was defined as [15]:

$$R_{th} = \frac{1}{2\pi k_f T_l} \cdot \ln\left(\frac{D_{ha} + 2T_t}{D_{ha}}\right) \quad (19)$$

k_f is the thermal conductivity of the fins material (aluminum alloy), with the value of 150 W/m^2·K [20].

The Number of Transfer Units (NTU) of the louvered fin radiator was calculated as [26]:

$$NTU = \frac{U_a A_a}{C_{\min}} \quad (20)$$

The heat transfer effectiveness of the radiator ε was evaluated with the general formula [26]:

$$\varepsilon = 1 - \exp\left\{\frac{NTU^{0.22}}{C_r}\left[\exp\left(-C_r \cdot NTU^{0.78}\right) - 1\right]\right\} \quad (21)$$

$C_r = C_{min}/C_{max}$ represents the heat capacity ratio, with the minimum and maximum heat capacity rates C_{min} and C_{max} defined as the lowest/highest value between the heat capacity rates of air and coolant, C_c and C_a (W/K) [20]:

$$C_c = m_c \cdot c_{p,c} \quad and \quad C_a = m_a \cdot c_{p,a} \quad (22)$$

m_a is the air mass flow rate (kg/s).

The total heat flux transferred from the hot side to the cold side of the radiator was calculated using the following expression [15, 27]:

$$Q_{rad} = \varepsilon N_T C_{\min}\left(T_{c,i} - T_{a,i}\right) \quad (23)$$

$T_{c,i}$ and $T_{a,i}$ are the inlet temperatures for the coolant and air fluxes inside the radiator.

3. Results and discussion

The louvered fin radiator is designed here to be included in a liquid cooling system for a PEMFC stack with gross electrical output power of 600 We, with stack voltage and current at full power of 21 V and 29 A, respectively [28]. The main design parameters of the cooling system are presented in Table 2.

Table 2. Design parameters for the cooling system for the PEMFC stack [28]

Parameter	Value
Maximum coolant flow rate	2 l/min
Maximum air velocity over surface radiator (cruise speed)	13.7 m/s
Maximum coolant temperature at the fuel cell outlet	343 K
Minimum coolant temperature at the fuel cell inlet	328 K
Minimum air temperature at the radiator exit	311 K

Based on the cooling system specifications from Table 2, we considered the following inlet temperatures for the coolant and air side: $T_{c,i}$ = 343 K, and $T_{a,i}$ = 298 K. The average temperatures at which we evaluated the fluid physical properties shown in Table 3 were selected as $T_{a,m}$ = 308 K and $T_{c,m}$ = 333 K.

Table 3. Physical properties for air and 50/50 water/glycol mixture

Fluid	$\rho_{a/c}$ (kg/m^3)	$\mu_{a/c}$ (kg/m·s)	$c_{p,a/c}$ (J/kg·K)	$k_{a/c}$ (W/m·K)
Air (a)	1.146	$1.89 \cdot 10^{-5}$	1006.7	0.0267
Water/ glycol (c)	1045	$1.05 \cdot 10^{-3}$	3490	0.39

The combined effect of fin pitch F_p (highest value), fin thickness F_t (lowest value), fin length F_l (second lowest) and louver pitch L_p (second lowest) generated the optimal (lowest) friction factor f for M2 model (see fig. 2.a). Due to the highest F_l, lowest L_p and second highest F_p, the f – factor of the M3 model was only about 14 % higher than that of the M2 model at similar Re_{Lh} values (Re_{Lh} > 200).

In the case of the Colburn j - factor evaluated for the M3 model, the second highest louver angle L_a and the lowest louver pitch L_p compensated with relative success the negative contribution of other geometrical parameters, like F_p, F_l, L_l and T_d (see Table 1). Instead, model M1 had the lowest F_p and F_l values and the highest L_p value, which overcame the limitations imposed by the lowest L_a and second highest T_d values and presented the optimal j-factor from all the models investigated (see Fig. 2.b). For example, at Re_{Lh} = 400, the j-factor of the model M1 was about 11 % higher than that of the M3 model.

Figure 3 presents the evolution of the surface goodness factor *"j/f"* ratio under the variation of Reynolds number Re_{Lp} for all the models investigated. We can see here that the M3 model showed the highest goodness factor along the entire Re_{Lp} domain. At Re_{Lp} = 400, the goodness factor of the model M1 was about 14 % higher than that of the M1 model.

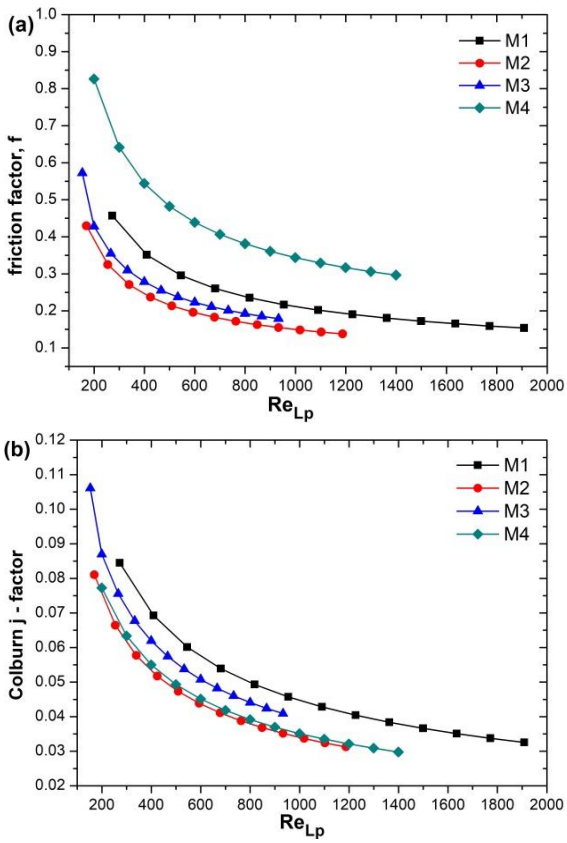

Figure 2. Variations of (a) f - factor and b) j - factor versus Re_{Lp} for the radiator models M1 – M4

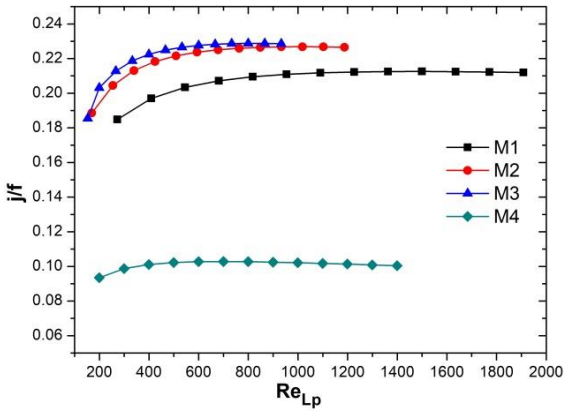

Figure 3. Surface goodness factor j/f variation for the radiator models M1 – M4

At this point of discussion, we need to better understand the relation between the j-factor, Re_{Lp}, and frontal air velocity V_a for a clear interpretation of the heat transfer coefficient h_a at the air side of the radiator. Figure 4 represents both the variations of the Re_{Lp} and h_a versus frontal air velocity.

The j – factor represents the main contribution to the h_a coefficient, calculated for specific Re_{Lp} values different from one model to another (see Fig. 4.a) due to a different louver pitch dimension. For example, at V_a = 5 m/s, j – factor was 0.054 for M1 model (Re_{Lp} = 681.5) and 0.068 for M3 model (Re_{Lp} = 333.2).

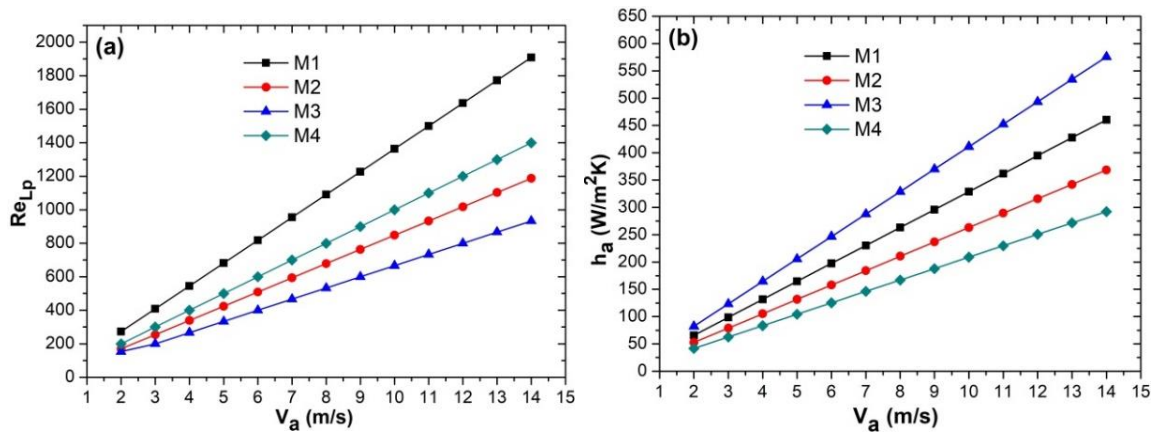

Figure 4. Evolution of the (a) louver pitch–based Reynolds number and (b) air-side heat transfer coefficient at different air velocities for models M1 – M4

Consequently, as we can see in Fig. 4.b, the heat transfer coefficient will have the maximum values in the case of model M3. For example, at V_a = 5m/s, h_a had a value of 205.6 W/m^{2}K for model M3 and of 164.5 W/m^2·K for model M1.

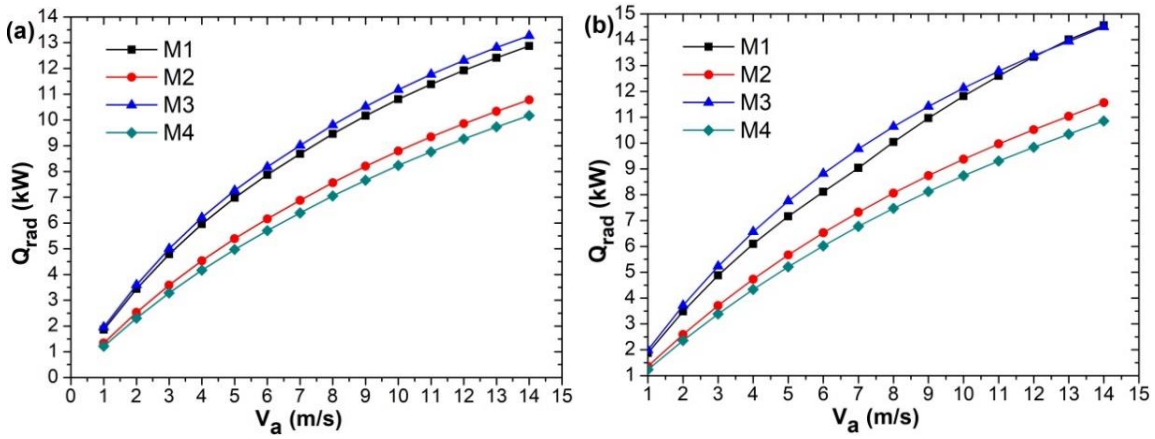

Figure 5. Heat rejection rate variation against the air velocity for the radiator models M1 – M4 at two different coolant flow rates: a) m_c = 1 l/min and b) m_c = 2 l/min

After increasing the coolant flow rate m_c from 1 l/min to 2 l/min, the difference between the heat rejection rates Q_{rad} presented by the models M1 and M3 at V_a values between 12 and 14 m/s became almost negligible (see Fig. 5.a and Fig. 5.b). At constant air velocity V_a = 5 m/s, between the two different coolant flow rates, Q_{rad} for M3 model increased by 2.6 %. Instead, when V_a rose from 5 to 6 m/s at m_c = 1 l/min, Q_{rad} was enhanced by 12.8 %, whereas at m_c = 2 l/min, Q_{rad} increased by 11.5 %.

So, the increase in air flow rate had a more significant influence on heat rejection rate than increasing coolant flow rate. D. Govindaj reported a similar behavior in his experimental wind tunnel testing of a louvered fin heat exchanger at air flow rates between 6 and 12 m/s [29].

4. Conclusions

This paper investigates the friction f – factor, the Colburn j – factor, the heat transfer coefficient and the heat rejection rate through specific correlations using four different heat exchanger models with louvered fins and flat tubes.

Model M3 with the highest fin length to fin pitch ratio F_l/F_p = 5.3, lowest louver pitch to fin pitch ratio L_p/F_p = 0.61, in correlation with the lowest louver length L_l = 6.8 mm and second highest louver angle L_a = 25.5 º presented the optimal thermo – hydraulic performance. The surface goodness factor j/f was 4% and 1.3% higher than that of the M2 model at louver pitch–based Reynolds numbers Re_{Lp} of 260 and 932, respectively.

The heat transfer coefficient on the air side h_a presented by the M3 model at frontal air velocities V_a between 2 and 14 m/s was about 20 – 25 % higher compared with model M1, having the second-best h_a values.

The heat rejection rate Q_{rad} attained the highest values in the case of the M3 model for a coolant flow rate m_c = 1 l/min. Instead, for m_c = 2 l/min, models M1 and M3 presented almost identical Q_{rad} values along the last three V_a values considered.

Conflict of interest

The author declares that he has no conflict of interest.

References

[1]. A. González, O. Ruz, E. Castillo, Numerical study of the fluid dynamics and heat transfer for shear-thinning nanofluids in a micro pin-fin heat sink,

Case Studies in Thermal Engineering 28 (2021) 101635-101662. Doi: 10.1016/j.csite.2021.101635

[2]. Q. Zuoqin, W. Qiang, C. Junlin, D. Jun, Simulation investigation on inlet velocity profile and configuration parameters of louver fin, Applied Thermal Engineering 138 (2018) 173–182. Doi: 10.1016/j.applthermaleng.2018.02.009

[3]. A. Sadeghianjahromi, C.C. Wang, Heat transfer enhancement in fin-and tube heat exchangers – a review on different mechanisms, Renewable and Sustainable Energy Reviews 137 (2021) 110470-110512. Doi: 10.1016/j.rser.2020.110470

[4]. S.H. Habibian, A.M.A. Abolmaali, Numerical investigation of the effects of fin shape, antifreeze and nanoparticles on the performance of compact finned-tube heat exchangers for automobile radiator, Applied Thermal Engineering 133 (2018) 248–260.
Doi: 10.1016/j.applthermaleng.2018.01.032

[5]. C.C. Wang, K.Y. Chen, J.S. Liaw, C.Y. Tseng, An experimental study of the air-side performance of fin-and-tube heat exchangers having plain, louver, and semi-dimple vortex generator configuration, International Journal of Heat and Mass Transfer 80 (2015) 281–287.
Doi: 10.1016/j.ijheatmasstransfer.2014.09.030

[6]. J.Y. Jang, C.C. Chen, Optimization of louvered-fin heat exchanger with variable louver angles, Applied Thermal Engineering 91 (2015) 138–150. Doi: 10.1016/j.applthermaleng.2015.08.009

[7]. J.S. Park, J. Kim, K.S. Lee, Thermal and drainage performance of a louvered fin heat exchanger according to heat exchanger inclination angle under frosting and defrosting conditions, International Journal of Heat and Mass Transfer 108 (2017) 1335–1339.
Doi: 10.1016/j.ijheatmasstransfer.2017.01.043

[8]. A. Okbaz, A. Pınarbas, A.B. Olcay, Experimental investigation of effect of different tube row-numbers, fin pitches and operating conditions on thermal and hydraulic performances of louvered and wavy finned heat exchangers, International Journal of Thermal Sciences 151 (2020) 106256. Doi: 10.1016/j.ijthermalsci.2019.106256

[9]. Z. Qi, J. Chen, Z. Chen, Parametric study on the performance of a heat exchanger with corrugated louvered fins, Applied Thermal Engineering 27 (2007) 539–544.
Doi: 10.1016/j.applthermaleng.2006.06.015

[10]. A. Okbaz, A. Pınarbası , A.B. Olcay, M.H. Aksoy, An experimental, computational and flow visualization study on the air-side thermal and hydraulic performance of louvered fin and round tube heat exchangers, International Journal of Heat and Mass Transfer 121 (2018) 153–169. Doi: 10.1016/j.ijheatmasstransfer.2017.12.127

[11]. P. Karthik, V. Kumaresan, R. Velraj, Experimental and parametric studies of a louvered fin and flat tube compact heat exchanger using computational fluid dynamics, Alexandria Engineering Journal 54 (2015) 905-915. Doi: 10.1016/j.aej.2015.08.003

[12]. J. Dong, J. Chen, Z. Chen, W. Zhang, Y. Zhou, Heat transfer and pressure drop correlations for the multi-louvered fin compact heat exchangers, Energy Conversion and Management. 48 (2007) 1506–1515.
Doi: 10.1016/j.enconman.2006.11.023

[13]. D. Ryan, J. Shang, Q. Quillivic, B. Porter, Performance and energy efficiency testing of a lightweight FCEV hybrid vehicle, European Electrical Vehicle Congress (EEVC), Brussels, Belgium, 3rd – 5th December 2014, 1 – 12.

[14]. K. Ikeya, K. Hirota, Y. Takada, T. Eguchi, K. Mizutani, T. Ohta, Development and evaluation of air-cooled fuel cell scooter, SAE Technical Paper 2011-32-0644 (2011) 1-9. Doi: 10.4271/2011-32-0644.

[15]. A. Fly, R.H. Thring, A comparison of evaporative and liquid cooling methods for fuel cell vehicles, International Journal of Hydrogen Energy 41 (2016) 14217 – 14229.
Doi: 10.1016/j.ijhydene.2016.06.089

[16]. L.B. Erbay, B. Doğan, M.M. Öztürk, in: S.M.S. Murshed and M.M. Lopes (Eds), Chapter 4: Comprehensive Study of Heat Exchangers with Louvered Fins, Heat Exchangers - Advanced Features and Applications, InTech (2017) 62 – 92. Doi: 10.5772/66472

[17]. D. Jung, D.N. Assanis, Numerical modeling of cross flow compact heat exchanger with louvered fins using thermal resistance concept, SAE Technical Paper 2006-01-0726 (2006) 1- 10. Doi: 10.4271/2006-01-0726.

[18]. V. Gnielinski, G1 heat transfer in pipe flow, VDI Heat Atlas. VDI-Buch. Springer, Berlin, Heidelberg, 2010. Doi: 10.1007/978-3-540-77877-6_34

[19]. Z. Said, M.E.H. Assad, A.A. Hachicha, E. Bellos, M.A. Abdelkareem, D.Z. Alazaizeh, B.A.A. Yousef, Enhancing the performance of automotive radiators using nanofluids, Renewable and Sustainable Energy Reviews 112 (2019) 183–194. Doi: 10.1016/j.rser.2019.05.052

[20]. H. Kwon, S. Park, J. Choi, J. Han, A Study on the Optimization of the Louver Fin Heat Exchanger for Fuel Cell Electric Vehicle Using Genetic Algorithm, Applied Science 13 (2023) 2539 -2553. Doi: 10.3390/app13042539

[21]. Y.-J. Chang, C.-C. Wang, A Generalized Heat transfer Correlation for Louver Fin Geometry, International Journal of Heat and Mass Transfer 40 (1997) 533-544. Doi: 10.1016/0017-9310(96)00116-0

[22]. H.C. Kang, G.W. Jun, Heat Transfer and Flow Resistance Characteristics of Louver Fin Geometry for Automobile Applications, Journal of Heat Transfer 133 (2011) 101802 – 101808. Doi: 10.1115/1.4004169

[23]. R.K. Shah, D.P. Sekulic, Fundamentals of heat exchanger design. John Wiley & Sons Inc., New Jersey, 2003.

[24]. Y.J. Chang, K.C. Hsu, Y.T. Lin, C.C. Wang, A generalized friction correlation for louver fin geometry, International Journal of Heat and Mass Transfer 12 (2000) 2237–2243. Doi: 10.1016/0017-9310(96)00116-0

[25]. W. Kays, A.L. London, Compact Heat Exchangers, 3rd Ed., McGraw – Hill Book Company, New York, 1984, p.15.
[26]. M.H. Kim, C.W. Bullard, Air-side thermal hydraulic performance of multi-louvered fin aluminum heat exchangers, International Journal of Refrigeration 25 (2002) 390–400. Doi: 10.1016/S0140-7007(01)00025-1.
[27]. É. Nogueira, Entropy generation analysis in a gasket plate heat exchanger using non-spherical shape of alumina boehmite nanoparticles, Ovidius University Annals of Chemistry 33 (2022) 41 – 49. Doi: 10.2478/auoc-2022-0006
[28]. R.O. Stroman, M.W. Schuette, G. S. Page, Cooling System Design for PEM Fuel Cell Powered Air Vehicles, Naval Research Laboratory Washington, DC 20375-5320, NRL/MR/6110--10-9253, 2010.
[29]. D. Govindaraj, Effective Selection Methodology for a Louvered Fin Heat Exchanger Using Thermal Resistance and Number of Transfer Units Method, SAE Technical Paper 2011-26-0090 (2011) 1-7 . Doi: 10.4271/2011-26-0090.

Received: 14.07.2024
Received in revised form: 08.09.2024
Accepted: 21.09.2024